Functions of neuronal Synaptobrevin in the post-Golgi transport of Rhodopsin in *Drosophila* photoreceptors

Hitomi Yamashita[¶], Yuka Ochi[¶], Yumi Yamada, Shogo Sasaki, Tatsuya Tago, Takunori Satoh, and Akiko K. Satoh[*]

Program of Life and Environmental Science, Graduate School of Integral Science for Life, Hiroshima University, 1-7-1 Kagamiyama, Higashi-Hiroshima, Hiroshima 739-8521, Japan

[*]Corresponding author
Akiko K. Satoh
Email: aksatoh@hiroshima-u.ac.jp
[‡]These authors contributed equally to this work.

Keywords: SNARE, Synaptobrevin, apical, recycling, photoreceptors, Rh1, *Drosophila*

SUMMARY STATEMENT

Newly synthesized rhodopsin merges with light-dependently internalized rhodopsin, and they are transported together to the photoreceptive membrane, rhabdomeres by Rab11/Rip11/MyoV complex and nSyb.

ABSTRACT

Polarized transport is essential for constructing multiple plasma membrane domains in the cell. *Drosophila* photoreceptors are an excellent model system to study the mechanisms of polarized transport. Rab11 is the key factor regulating the post-Golgi transport of rhodopsin 1 (Rh1), a photoreceptive protein, to the rhabdomere, a photoreceptive plasma membrane. Here, we found that neuronal Synaptobrevin (nSyb) colocalizes with Rab11 on the trans-side of Golgi stacks and post-Golgi vesicles at the rhabdomere-base, and nSyb-deficiency impairs rhabdomeric transport and induces accumulation of Rh1 and vesicles in the cytoplasm; this is similar to the effects of Rab11 loss. These results indicate that nSyb acts as a post-Golgi SNARE toward

rhabdomeres. Surprisingly, in Rab11-, Rip11-, and nSyb-deficient photoreceptors, illumination enhances cytoplasmic accumulation of Rh1 colocalizing with Rab11, Rabenosyn5, nSyb, and Arrestin 1 (Arr1). Arr1 loss but not Rab5 dominant negative (Rab5DN) protein expression inhibits the light enhanced cytoplasmic Rh1 accumulation. Rab5DN inhibits the generation of Rh1 containing multi-vesicle bodies rather than Rh1 internalization. Overall, these results indicate that exocytic Rh1 mingle with endocytosed Rh1 and are then transported together to rhabdomeres.

INTRODUCTION

The Golgi apparatus is the central organelle in the secretory pathway. The basic structural unit of the Golgi apparatus is the Golgi stack, which comprises several flattened membrane-enclosed compartments, called cisternae, and tubules. The Golgi stack itself is structurally polarized; the “cis” face receives newly synthesized secretory proteins/lipids from the endoplasmic reticulum (ER) and the “trans” face sorts and sends them to multiple destinations within the cell (Klumperman, 2011; Papanikou and Glick, 2014). Earlier, recycling endosomes (RE) were defined as perinuclear compartments where endocytosed materials transit before being recycled back to the plasma membrane (Goldenring, 2015; Mayor et al., 1993; Yamashiro and Maxfield, 1987). However, studies over the past decade have indicated that recycling endosomes receive newly synthesized proteins from Golgi stacks, en route to the plasma membrane (Ang et al., 2004; Lock and Stow, 2005; Misaki et al., 2010; Taguchi, 2013).

We recently reported that REs can exist in two distinct states — Golgi-associated REs (GA-REs) and free REs in *Drosophila*, microtubule-disrupted HeLa cells, and sea urchin embryos (Fujii et al., 2020a; Fujii et al., 2020b). GA-REs and free REs are interconvertible by detachment from and reattachment to Golgi stacks. Glycosylphosphatidylinositol-anchored cargo protein (GPI-AP) but not vesicular stomatitis virus G protein (VSV-G) travels through GA-REs and free REs before reaching the plasma membrane in HeLa cells (Fujii et al., 2020a). Thus, the interchange of GA-REs and free REs could be responsible for post-Golgi transport. Among *Drosophila* photoreceptors, Rab11, one of the most studied RE markers, is essential for the post-Golgi transport of rhodopsin, Rh1 (Satoh et al., 2005). Rab11 localizes on the

trans-side of Golgi stacks (GA-RE) and post-Golgi vesicles bearing Rh1 at the base of rhabdomeres (free RE).

Recently, we showed that another well-characterized RE marker, human Vamp3, and its fly ortholog, Synaptobrevin (Syb), localize on the trans-side of Golgi stacks in fly photoreceptors and salivary glands (Fujii et al., 2020a). Vamp3 and Syb belong to a family of molecules known as SNAREs (soluble *N*-ethylmaleimide-sensitive factor attachment protein receptors). SNAREs are small C-terminally anchored proteins with a highly conserved domain termed the SNARE motif. The spontaneous assembly of four complementary SNARE motifs results in a tight connection between the two membranes and drives their fusion. Vamp3/Syb is reported to be required for the fusion of constitutive secretory carriers with the plasma membrane (Gordon et al., 2017), ecdysone secretion (Yamanaka et al., 2015), transcytosis of Wingless (Yamazaki et al., 2016), and patched placement at the contact site in cytonemes (González-Méndez et al., 2020). In addition to Syb, the closely related neural Synaptobrevin (nSyb) is expressed only in neural cells. nSyb, together with Syx1A and Snap24, regulates synaptic vesicle fusion (Deitcher et al., 1998; DiAntonio et al., 1993; Haberman et al., 2012; Jin et al., 2018; Rister and Heisenberg, 2006; Wang et al., 2014a; Yoshihara et al., 1999). nSyb is also involved in neuron-specific endomembrane degradation (Haberman et al., 2012; Jin et al., 2018; Wang et al., 2014a; Wang and Hiesinger, 2012). nSyb has redundant functions with Syb in synaptic vesicle fusion and cell viability (Bhattacharya et al., 2002).

In this study, we investigated whether Syb and neuron-specific nSyb are involved in Rh1 transport. We found nSyb is essential for Rh1 transport to the rhabdomeres and Syb can compensate for the loss of nSyb. Syx5 (Kondylis and Rabouille, 2003; Satoh et al., 2016), Sec22 (Zhao et al., 2015), and Gos28 (Rosenbaum et al., 2014) are identified as SNAREs involved in Rh1 transport from ER to Golgi or within Golgi stacks, however, the SNAREs involved in the post-Golgi transport of Rh1 remain unknown. Therefore, we aimed to identify the SNAREs involved in the post-Golgi transport of Rh1 in fly photoreceptors. Thus, this is the first report to identify SNAREs involved in the post-Golgi transport of Rh1 in fly photoreceptors. We also found that newly synthesized exocytic Rh1 merges with light-dependently internalized Rh1 from the rhabdomeres. These Rh1 seems likely to be recycled back to the rhabdomeres by Rab11/Rip11/MyoV complex and nSyb.

RESULTS

Rh1 transport is impaired in nSyb-deficient photoreceptors

To understand whether Syb is necessary for the post-Golgi transport of Rh1, we investigated the phenotypes of the photoreceptor-carrying homozygous Syb null alleles, *Syb*$^{21\text{-}15}$ and *Syb*$^{25\text{-}77}$. As both alleles are lethal, we used the FLP/FRT method (Xu and Rubin, 1993) to prepare mosaic retinas, which contain both the wild-type and Syb null homozygous photoreceptors. In these mosaic retinas, most photoreceptors were wild-type cells marked by RFP, but some small patches of RFP-negative-*Syb*$^{21\text{-}15}$ or *Syb*$^{25\text{-}77}$ homozygous clones were observed. In homozygous Syb null photoreceptors as well as wild-type photoreceptors, Rh1 localized to the rhabdomere appeared as oval in the cross-section, forming a tight bundle of photoreceptive microvilli protruding from the apical membrane into the central lumen of the ommatidium (Fig. 1A, B, H). Na^+/K^+-ATPase is localized on the basolateral membrane, which outlines photoreceptors. Na^+/K^+-ATPase localization and cell shapes are normal in *Syb*$^{21\text{-}15}$ and *Syb*$^{25\text{-}77}$ homozygous photoreceptors (Fig. 1A, B). Thus, despite cell-lethality of *Syb*$^{21\text{-}15}$ and *Syb*$^{25\text{-}77}$ homozygous photoreceptors, loss of Syb does not impact photoreceptor development.

As photoreceptors express nSyb, which has redundant functions with Syb in synaptic vesicle fusion and cell viability (Bhattacharya et al., 2002), we wondered whether nSyb and Syb would also have redundant functions in membrane trafficking to the rhabdomeres. Thus, we examined the phenotypes of nSyb-deficient photoreceptors. In mosaic retinas with both the wild-type and the null mutation, *nSyb*$^{\Delta F33B}$ homozygous photoreceptors, *nSyb*$^{\Delta F33B}$ homozygous clones were not small, suggesting complete loss of nSyb is not cell-lethal. However, Rh1 is accumulated in the cytoplasm of *nSyb*$^{\Delta F33B}$ homozygous photoreceptors (Fig. 1C, H). We also found that *nSyb*^{d02894} homozygous photoreceptors with a 5′-P-element insertional mutation could accumulate Rh1 in the cytoplasm (Fig. 1D, H). On the contrary, the homozygous photoreceptors with the *nSyb*$^{d02894\text{ex}1}$ allele, made by precise excision, showed normal localization of Rh1 in the rhabdomeres (Fig. 1E, H). Na^+/K^+-ATPase localization and cell shapes were normal in *nSyb*$^{\Delta F33B}$ and *nSyb*^{d02894} homozygous photoreceptors (Fig. 1C, D). These results strongly indicate that nSyb is essential for Rh1 transport to rhabdomeres. To investigate the redundancy between Syb and nSyb, we first examined Rh1 accumulation in *nSyb*$^{\Delta F33B}$ homozygous photoreceptors with a single *Syb*$^{21\text{-}15}$ chromosome: these cells show massive Rh1 accumulation in the cytoplasm, but this accumulation is not

significantly more severe than that in *nSyb*$^{\Delta F33B}$ homozygous photoreceptors (Fig. 1F, H). On the contrary, *nSyb*$^{\Delta F33B}$ homozygous photoreceptors expressing FLAG::Syb display normal Rh1 localization in the rhabdomeres (Fig. 1G, H), indicating that Syb and nSyb function redundantly in Rh1 transport.

To investigate the detailed phenotype of *nSyb*$^{\Delta F33B}$ homozygous photoreceptors, we observed thin sections of pupal photoreceptors using electron microscopy (Fig1. I, J). *nSyb*$^{\Delta F33B}$ homozygous photoreceptors accumulate a lot of abnormal vesicles in the cytoplasm. These vesicles appear empty with irregular profiles; they are typically 200 nm across and substantially larger than normal secretory vesicles. These are indistinguishable with vesicles accumulating in photoreceptors that are deficient for Rab11/Rip11/MyoV complex or exocyst complex involved in post-Golgi transport to rhabdomeres (Fig. I, J) (Beronja et al., 2005; Laffafian and Tepass, 2019; Li et al., 2007; Satoh et al., 2005). Thus, these results indicate that Syb and nSyb are involved in the post-Golgi transport of Rh1 in *Drosophila* photoreceptors.

Syb and nSyb are localized on early endosomes, the trans-side of Golgi stacks, and post-Golgi vesicles at the base of rhabdomeres

We next investigated the localization of Syb and nSyb. As the phenotypes in nSyb null photoreceptors are quite well resemble to those of deficient in one of the components among Rab11/Rip11/MyoV complex, we first examined whether Syb and nSyb colocalize with Rab11 on post-Golgi vesicles at the base of rhabdomeres. FLAG::Syb and HA::nSyb are driven by Rh1-Gal4, which is activated in the late pupal stage. In fact, both FLAG::Syb and HA::nSyb colocalize with Rab11 at the base of rhabdomeres (Fig. 2A arrows), however, we found some foci that were FLAG::Syb and HA::nSyb positive but Rab11-negative in areas distant from the rhabdomeres (Fig. 2A arrowheads). As nSyb is reported to be localized on the endosomes in photoreceptor axons (Haberman et al., 2012; Jin et al., 2018), we investigated the relationship between FLAG::Syb/HA::nSyb and early endosome markers, Rab5/Rabenosin5 (Rbsn5) in the region under the rhabdomeres. We found that both FLAG::Syb and HA::nSyb colocalize with Rbsn5 (Fig. 2B arrows). They are also colocalized with EGFP::Rab5 (Fig. 2D, H arrowheads). Thus, FLAG::Syb and HA::nSyb localize on early endosomes in the cell body of photoreceptors.

There are still some foci stained with FLAG::Syb or HA::nSyb without Rab5/Rbsn5, apart from the rhabdomeres. Rab11 is localized on post-Golgi vesicles in free REs, as well as on the trans-side of Golgi stacks in GA-REs. Thus, we next investigated whether FLAG::Syb and HA::nSyb localize in the peripheral region of Golgi stacks. We found that both FLAG::Syb and HA::nSyb colocalized with Rab6 puncta in the photoreceptor cytoplasm (Fig. 2C-F, H arrows) presumably on the trans-side of Golgi stacks. To investigate the detailed localization of FLAG::Syb and HA::nSyb within the Golgi stacks/GA-RE complex, we simultaneously compared these protein localizations with two other markers in the Golgi stacks/GA-RE complex. Both FLAG::Syb and HA::nSyb signals were detected on the trans-side of Golgi stacks and were separated from both the cis-Golgi marker GM130 and αCOP (Fig. 2E, I). FLAG::Syb was well overlapped with Rab6 but partially with Rab11 (Fig. F, G), whereas HA::nSyb was localized between Rab6 and Rab11 (Fig. 2J). These results indicate that FLAG::Syb and HA::nSyb localize on the trans-side of Golgi stacks as GA-RE, post-Golgi vesicles as free RE, and early endosomes.

Light enhances Rh1 accumulation in nSyb-deficient photoreceptors

It is well known that photoactivated Rh1 is endocytosed (Orem et al., 2006; Satoh and Ready, 2005). As FLAG::Syb and HA::nSyb are localized to early endosomes, as well as GA-RE and free RE, we wondered whether Syb and nSyb are involved in the transport of internalized Rh1. Therefore, we first investigated the influence of light on the degree of Rh1 cytoplasmic accumulation in nSyb-deficient photoreceptors. Interestingly, Rh1 accumulation was greatly reduced in both $nSyb^{\Delta F33B}$ and $nSyb^{d02894}$ homozygous photoreceptors in the dark (Fig. 3 A, D, G, H). As Rh1 internalization depends on Rab5 and Arrestin1 (Arr1) (Kamalesh et al., 2017; Pinal and Pichaud, 2011; Satoh and Ready, 2005), we examined the effects of dominant-negative Rab5 protein, Rab5S43N, or arr1 null mutation on Rh1 accumulation in $nSyb^{\Delta F33B}$ and $nSyb^{d02894}$ homozygous photoreceptors. Rab5S43N expression did not affect Rh1 accumulation on both $nSyb^{\Delta F33B}$ and $nSyb^{d02894}$ homozygous photoreceptors, but arr1 null allele, $arr1^{1}$, notably suppressed Rh1 accumulation in $nSyb^{\Delta F33B}$ homozygous photoreceptors (Fig. 3B, C, E-H). These results suggest that part of Rh1 accumulated in the cytoplasm might be derived from rhabdomeres, and nSyb likely regulates endocytosed Rh1 transport, but it is difficult to explain why Rab5S43N does not impact Rh1 accumulation.

Light enhances Rh1 accumulation in Rab11- and Rip11-deficient photoreceptors

Next, we investigated how the components involved in post-Golgi transport to rhabdomeres, such as Rab11/Rip11/MyoV complex or exocyst complex regulate the transport of endocytosed Rh1. We examined the influence of light on the cytoplasmic accumulation of Rh1 in the absence of Rab11, Rip11, and Sec15, a subunit of the exocyst complex. We used the retinas expressing Rab11RNAi by longGMR-Gal4, because Rab11 null homozygous clones in the retinas are extremely small (Satoh et al., 2005). Massive cytoplasmic accumulation of Rh1 was observed in Rab11RNAi-expressing retinas dissected from flies reared in light conditions; however, Rh1 accumulation in the cytoplasm was greatly reduced in retinas dissected from dark-reared flies (Fig. 4A, B, K). Similar to Rab11-reduced photoreceptors, the $Rip11^{G0297}$ homozygous null photoreceptors accumulate Rh1 in the cytoplasm in light conditions, but not in the dark (Fig. 4C, D, K, L). In contrast, $Sec15^{1}$ homozygous null photoreceptors accumulate Rh1 in the cytoplasm in both light and dark conditions (Fig. 4G, H, K, L). We also found that Rab5S43N does not affect Rh1 accumulation in $Rip11^{G0297}$ and $Sec15^{1}$ homozygous photoreceptors (Fig. 4E, I, K, L), whereas $arr1^{1}$ reduces Rh1 accumulation in both mutant cells (Fig. 4F, J, K, L). In the case of $Rip11^{G0297}$ homozygous photoreceptors, this reduction was significant (Fig. 4L). These results suggest that at least the Rab11/Rip11/MyoV complex must regulate endocytosed Rh1 transport.

Rab5S43N does not inhibit endocytosis

Rab5S43N does not affect Rh1 accumulation, even though $arr1^{1}$ reduces Rh1 accumulation in photoreceptors under either nSyb or Rip11 deficiency. Therefore, we revisited the function of Rab5 in fly photoreceptors. In mammalian cells, Rab5 regulates the fusion of endocytic vesicles with early endosomes, and the homotypic fusion of early endosomes (Langemeyer et al., 2018; Wandinger-Ness and Zerial, 2014). We thus investigated the localization of Rab5 in detail, as well as the effect of Rab5S43N expression in fly photoreceptors. First, we compared the localization of EGFP::Rab5, Rbsn5, and Rab7 in wild-type photoreceptors (Fig. 5A). Rab7 signals are typically localized on the relatively large round organelle and are sometimes limited to its outlines, suggesting that Rab7 is expressed on the multivesicular bodies (MVBs) in fly photoreceptors (Fig. 5A). Rab7 is localized on the outlines of Rh1-containing large vesicles (RLVs), which we previously identified as MVBs (Fig. 5B arrows) (Satoh et al.,

2005). EGFP::Rab5 was found on RLV-like large vesicles with Rab7 and Rbsn5, but most of them were found on smaller vesicles, which were presumably early endosomes. EGFP::Rab5 and Rbsn5 were intensively colocalized on these vesicles (Fig. 5A arrowheads), whereas Rab7 joined them only occasionally (Fig. 5A arrows). We then investigated the effect of Rab5S43N and Rab7T22N on the existence of RLVs. Rab5S43N expression reduces, whereas Rab7T22N expression increases the number of RLVs (Fig. 5B, C arrows). These results suggest that Rab5S43N inhibits RLV formation or an earlier step.

Arr1 is required for light-dependent Rh1 endocytosis (Mu et al., 2019; Satoh and Ready, 2005). Arr1 localizes to the cytoplasm in the dark but translocates into the rhabdomeres under illumination (Fig. 5D) (Satoh and Ready, 2005; Shieh et al., 2014). Arr1 was mainly localized in the RLVs in retinas dissected from wild-type or Rab7T22N expressing flies reared in light (Fig. 5E arrows). On the contrary, Arr1 localized to the cytoplasm in Rab5S43N-expressing photoreceptors under illumination (Fig. 5E arrowheads). The pattern of Arr1 localization in light-reared Rab5S43N-expressing photoreceptors is different from that in dark-reared wild-type cells. Arr1 is not diffused but is concentrated near the rhabdomere. Using electron microscopy, we found that many small vesicles (100 nm or less in diameter) are accumulated under the rhabdomeres in Rab5S43N-expressing photoreceptors (Fig. 5G, H arrows). These results indicate that endocytic vesicles, which contain Rh1 endocytosed by Arr1, do not fuse, and then fail to form RLVs in Rab5S43N-expressing photoreceptors (Fig. 5F-H).

Rab11, Rbsn5, Arr1 and nSyb are localized on Rh1-bearing abnormal vesicles accumulated in post-Golgi transport-defective mutants

Suppression of Rh1 accumulation by *arr1*^{1} mutation in *nSyb*$^{\Delta F33B}$ and *Rip11*^{G0297} homozygous photoreceptors indicated that Rh1 accumulation in the cytoplasm originates from Golgi stacks as well as rhabdomeres. In other words, newly synthesized Rh1 can be accumulated in the cytoplasm together with endocytosed Rh1. To investigate this possibility, we examined whether cytoplasmic Rh1 colocalizes with the post-Golgi marker Rab11, and the endocytic markers, Rbsn5 and Arr1. Rab11 is strongly localized at the base of the rhabdomeres but is also detected in the cytoplasm together with Rh1 in *nSyb*$^{\Delta F33B}$, *Rip11*^{G0297}, and *Sec15*^{1} homozygous photoreceptors (Fig. 6A), indicating that some Rh1 is localized in post-Golgi vesicles. We also found that

both endocytic markers, Rbsn5 and Arr1, colocalize with Rh1 in the cytoplasm, indicating that some cytosolic Rh1 is endocytosed from the rhabdomeres in *nSyb*$^{\Delta F33B}$, *Rip11*^{G0297}, and *Sec15*^{1} homozygous photoreceptors (Fig. 6B, C). Finally, we investigated FLAG::Syb localization. We found that FLAG::Syb colocalizes with cytoplasmic Rh1 in *Rip11*^{G0297} and *Sec15*^{1} homozygous photoreceptors (Fig. 6D). These results strongly indicate that transport of both exocytic and endocytic Rh1 is inhibited and that Rh1 of either origin accumulates together in the cytoplasm in *nSyb*$^{\Delta F33B}$, *Rip11*^{G0297}, and *Sec15*^{1} homozygous photoreceptors.

Retromer is epistatic to nSyb in Rh1 recycling pathway

Previous studies have shown that endocytosed Rh1 is recycled back to rhabdomeres, and retromer is a key factor for this recycling process (Kamalesh et al., 2017; Thakur et al., 2016; Wang et al., 2014b; Xiong et al., 2012; Xiong and Bellen, 2013). Thus, we addressed the relationship between the functions of nSyb and retromer in Rh1 recycling. We first investigated the localization of a retromer subunit, Vps26. Vps26::V5 expressed by Rh1-Gal4 is well-colocalized with an early endosome marker, Rbsn5, under the rhabdomeres (Fig. 7A, B arrows). Vps26::V5 is also detected on RLVs (Fig. 7A arrowhead). The results indicate that retromers mainly localize on the early endosomes but also on MVBs. Homozygous photoreceptor phenotypes of Vps26 null allele, *Vps26*^{B} were then observed in pupal mosaic retinas. In Vps26 deficient photoreceptor cells, more Rh1 is detected in the cytoplasm than that in the wild-type photoreceptors, but this Rh1 accumulation is limited, compared to that in nSyb null photoreceptors (Fig. 1C, 7C, G). Interestingly, Rh1 cytoplasmic accumulation in nSyb null photoreceptors expressing Vps26RNAi is also lower than that in nSyb null photoreceptors, although this reduction is not significant (Fig. 1C, 7D, G). Similarly, in homozygous photoreceptors of a null allele for another retromer subunit of Vps35, *Vps35*^{HM20}, or either in *Vps35*^{HM20} homozygous photoreceptors expressing nSybRNAi, the accumulation of Rh1 in the cytoplasm is lower than that of nSyb null photoreceptors (Fig. 7E-G). Vps35 null mosaic retinas expressing nSybRNAi clearly showed a lower Rh1 accumulation in *Vps35*^{HM20} homozygous photoreceptors expressing nSybRNAi than in the wild-type photoreceptors expressing nSybRNAi by side-by-side comparison (Fig. 7F, G). These results indicate that retromer is epistatic to nSyb in the Rh1 recycling pathway.

DISCUSSION

In the present study, we found that nSyb is essential for Rh1 transport to rhabdomeres. This is the first report identifying the SNARE involved in the post-Golgi transport in fly photoreceptors. The role of nSyb in Rh1 transport was unanticipated, because nSyb, together with Syx1A and Snap25, is known to regulate synaptic vesicle fusion (Broadie et al., 1995; Deitcher et al., 1998; DiAntonio et al., 1993; Littleton et al., 1998; Rao et al., 2001; Yoshihara et al., 1999). As SNAREs are key factors for determining the specificity of fusion (Jahn and Scheller, 2006; Malsam et al., 2008), other SNAREs, different from Syx1A and Snap25, may be involved in the fusion of Rh1-bearing post-Golgi vesicles with rhabdomeres. Identifying these other SNARE members involved in Rh1 transport is thus vital for future studies. The involvement of Syb in Rh1 transport in late pupal photoreceptors on the wild-type background remains unclear. We have shown that Syb expression can rescue Rh1 transport in nSyb-deficient photoreceptors. Therefore, the ability of Syb to regulate Rh1 transport is confirmed, but it is unclear whether Syb is expressed in the photoreceptors in the late pupal stage. Indeed, Syb-deficient photoreceptors do not show cytoplasmic Rh1 accumulation. Thus, the amount of nSyb expressed in late pupal photoreceptors is considered sufficient to drive Rh1 transport.

The function of nSyb for Rh1 transport in fly photoreceptors is unexpected from another point of view: in biogenesis of the cilia-derived light-sensing rod outer segments (ROSs) in vertebrate photoreceptors, STX3, Snap25 and Vamp7 are SNAREs which mediate the fusion of rhodopsin-containing carriers to the plasma membrane. Rh1 transport in fly photoreceptors and rhodopsin transport in the vertebrate photoreceptors share several factors, such as Rab6, Rab11, Rab11FIP, and exocyst; however, there is no report of Synaptorevin2 involvement in rhodopsin transport (Deretic, 1997; Deretic et al., 1995; Deretic and Papermaster, 1993; Kakakhel et al., 2020; Kandachar et al., 2018; Mazelova et al., 2009). It would be important to study the function of orthologs of STX3, Snap25, and Vamp7 in fly photoreceptors.

Localization of nSyb and Syb is not limited to GA-REs and free REs, which are involved in the exocytic pathway; they are also concentrated in early endosomes with Rab5 and Rbsn5. Together with the strong light- and Arr1-dependence of Rh1 accumulation in *nSyb*$^{\Delta F33B}$ homozygous photoreceptors, our results indicate that Rh1 accumulated in the cytoplasm originates from Golgi stacks as well as rhabdomeres by

light-dependent endocytosis. In the past decade, detailed studies by several fly labs have revealed several important factors involved in the post-Golgi transport of Rh1 toward rhabdomeres. Lack of these factors always shows similar phenotypes to nSyb deficiency including accumulation of Rh1 and abnormal vesicles in photoreceptor cytoplasm (Fig. 7) (Beronja et al., 2005; Hebbar et al., 2020; Laffafian and Tepass, 2019; Li et al., 2007; Otsuka et al., 2019; Pocha et al., 2011; Satoh et al., 2005). This cytoplasmic accumulation of Rh1 supposedly originates from Golgi stacks. Indeed, newly synthesized Rh1 is confirmed to originate from Golgi stacks based on Rh1 transport assays (Satoh et al., 2005). However, in this study, we showed that some portion of accumulated Rh1 is delivered from rhabdomeres by light-dependent endocytosis, at least in cases of Rab11 or Rip11 deficiencies. We also showed that Rh1 and abnormal vesicles accumulated in the cytoplasm are positive for Rab11, Rbsn5, and Arr1, indicating that they have the nature of post-Golgi vesicles and early endosomes. These results imply that exocytic and endocytic Rh1 merge on GA-REs, free REs, or early endosomes; further, Rh1 from both origins is transported to rhabdomeres by common factors, which were previously postulated to be involved in only post-Golgi transport. We assumed that nSyb regulates the final fusion of Rh1-bearing vesicles with the plasma membrane at the base of the rhabdomeres because of the strong similarity of Rh1-bearing vesicles accumulating in nSyb-deficient photoreceptors, in comparison to those in the deficient photoreceptors of one of the components of Rab11/dRip11/MyoV or exocyst complex. However, the possibility that nSyb regulates the fusion to converge exocytic and endocytic pathways is not excluded.

It is well known that endocytosed Rh1 degrades for sensitization and prevention of retinal degeneration (Acharya et al., 2004; Alloway et al., 2000; Chinchore et al., 2009; Han et al., 2007; Kiselev et al., 2000; Orem et al., 2006; Xu et al., 1998; Yonamine et al., 2011). However, several studies have shown that endocytosed Rh1 is also recycled back to rhabdomeres (Kamalesh et al., 2017; Thakur et al., 2016; Wang et al., 2014b; Xiong et al., 2012; Xiong and Bellen, 2013). Retromer is reported to be a key factor for Rh1 recycling in adult photoreceptors, and a lack of retromer induces light-dependent retinal degeneration (Kamalesh et al., 2017; Wang et al., 2014b). Thus, Rh1 recycling is essential for photoreceptor viability. However, retromer deficiency does not impact Rh1 transport in the late pupal stage (Wang et al., 2014b). We confirmed that the lack of retromer subunit in pupal photoreceptors induces

mild cytoplasmic Rh1 accumulation. Analysis of genetic interaction between nSyb and retromer showed that retromer is epistatic to nSyb. nSyb and retromer double mutant photoreceptors shows a mild cytoplasmic accumulation of Rh1, similar to retromer single mutation rather than nSyb single mutation. Such epistatic relation of nSyb and retromer can be interpreted in two ways: nSyb functions in the later step of transport in comparison to that of the retromer (for example, TGN/RE to the rhabdomeres vs early endosome to TGN/RE), or the retromer and nSyb function on the budding and fusion processes of the same step of vesicle transport.

It is puzzling that Rh1 is endocytosed and recycled back to the rhabdomeres. One of the possible reasons for this phenomenon could be related to quality control: light-damaged Rh1 could be selectively sent to the late endosomes and degraded, whereas, unaffected Rh1 is sent back to the rhabdomeres. The other possibility is that this recycling process might give the additional regulatory system to regulate the amount of Rh1 in the rhabdomeres. In fact, Rab11 activity is regulated by light-stimulation through Crag (Xiong et al., 2012); therefore, the endocytosed-pool could contribute to control the amount of rhabdomeric Rh1 responsible for phototransduction.

MATERIALS AND METHODS

Drosophila stocks and genetic background

Fruit flies were grown at 20–25 °C on standard cornmeal–glucose–agar–yeast medium either in the laboratory with room light or incubator without light. The following fly stocks were used: Rh1-Gal4 (Dr. Hama, Kyoto Sangyo University, Japan), longGMR-Gal4 (Bloomington Drosophila Stock Center No. 8605, Bloomington, IN, USA; indicated as BL8605 in the following stocks), coinFLP-Gal4 (BL58751), UAS-Rab11RNAi^{pWIZ,} (Satoh et al., 2005), nSyb^{d02894}/TM6B, Tb^{1} (BL19183), nSyb$^{\Delta F33B}$ /TM3 (BL51621), Syb$^{21-15}$/CyO (BL9873), Syb$^{25-77}$/CyO (BL9874), arr1^{1}/SM6b (BL42253), UAS-EGFP::Rab5 (BL43336), Rip11^{G0297} FRT19A (Kyoto Drosophila Stock Center No. 111918, Kyoto, Japan; indicated as KY111918 in the following stocks), FRT82B Sec15^{1}/TM3GFP (BL24889), UAS-Rab5S43N (BL427903, BL427904), UAS-Rab7T22N (Dr. Emery, University of Montreal, Canada), UAS-Vps26RNAi^{HMS01768} (BL38937), UAS-nSybRNAi^{JFS03417} (BL31983), UAS-Vps26::V5 (BL67148), Vps26^{B},

FRT19A/FM7 (BL57140), FRT42D, Vps35^{HM20}/CyO (BL67202), UAS-HA::nSyb (produced in the present study) and UAS-FLAG::Syb (produced in the present study).

nSyb^{d02894} and nSyb$^{\Delta F33B}$ were combined with FRT80B, and Syb$^{21-15}$ and Syb$^{25-77}$ were combined with FRT42D to make mosaic by FLP/FRT method (Xu and Rubin, 1993). Males of nSyb^{d02894} FRT80B/TM6B were crossed to females of delta 2-3 line (KY107139) to obtain nSyb$^{d02894\ ex1}$ FRT80B/TM6B.

Males of FRT42D Syb$^{21-15}$/CyOGFP or FRT42D Syb$^{25-77}$/CyOGFP were crossed to y w eyFLP; FRT42D RFP to make mosaic eyes. Males of nSyb^{d02894} FRT80B/TM6B, nSyb$^{d02894\ ex1}$ FRT80B/TM6B or nSyb$^{\Delta F33B}$ FRT80B/TM6B were crossed to y w eyFLP;; RFP FRT80B to make mosaic eyes.

Transgenic flies for UAS-HA::nSyb and UAS-FLAG::Syb

A P-element vector, pPdM-UAST was constructed from pUAST, by deleting MluI-site upstream of UAST promoter, then replaced from EcoRI-site to XbaI-site with a DNA fragment (5'-GAATTCGGGGATCTAGATCGGGGTACCGCCACCATGTACCCATACGATGTTCCTGACTATACTAGTGGAGGAGGAGGTTCTGGTGGTGGTGCGGCCGCTGGTGGTAGATCTGGTGGTGGCGCGCCTGGTGGTGGAGGTTCTGGTGGCGGTGGCTCGAGTGAGCAAAAGCTCATTTCTGAAGAGGACTTGTAAGGGCCCTTCGAAGGTAAGCCTATCCCTAACCCTCTCCTCGGTCTCGATTCTACGCGTACCGGTCATCATCACCATCTAGA-3') encoding a N-terminus HA-tag (MYPYDVPDY), linker (TSGGGGSGGGAAAGGRSGGGAPGGGGSGGGGSS), and C-terminus Myc-tag (EQKLISEEDL*). The entire coding regions of an isoform of nSyb, nSyb-RA, was amplified from cDNA of *w*^{1118} 3rd instar larvae, then cloned between XhoI and XbaI site of pPdM-UAST, resulting pUAS-HA::nSyb. To build pUAST-FLAG-Syb, 2.2kbp DNA fragment containg entire coding region and introns of all isoforms of Syb was amplified from *w*^{1118} genomic DNA, then cloned into pUAST, together with N-terminus 3xFLAG tag. Plasmids were injected into *w*^{1118} embryos to generate transgenic lines.

Immunohistochemistry

Fixation and staining were performed as described previously except fixative (Satoh and Ready, 2005). PLP (10mM periodate, 75mM Lysine, 30mM phosphate buffer,

4%paraformaldehyde) was used as fixative. The primary antisera used were as follows: rabbit anti-Rh1 (1:1000) (Satoh et al., 2005), chicken anti-Rh1 (1:1000) (Satoh et al., 2013), mouse monoclonal anti-Na^+/K^+-ATPase-α subunit (1:500 ascites) (Developmental Studies Hybridoma Bank (DSHB), Iowa City, IA, USA), rat anti-Rab11 (1:250) (Otsuka et al., 2019), guinea pig anti-Rab6 (1:300) (Iwanami et al., 2016), rat anti-Rbsn5 (1:300) (a gift from Dr. Nakamura, Kumamoto University, Kumamoto, Japan), rabbit anti-Rab7 (1:300) (a gift from Dr. Nakamura, Kumamoto University, Kumamoto, Japan), rabbit anti-Arr1 (a gift from Dr. Dolph, Dartmouth College, UAS), guinea pig anti-αCOP (1:300) (a gift from Dr. Inoue Kyoo Institute of Technology, Kyoto, Japan), rabbit anti-GM130 (1:300) (Abcam, Cambridge, UK), rabbit anti-MPPE (1:1000) (a gift from Dr. Han, Southeast University, Nanjing, China), rabbit anti-HA (1:300) (Medical and Biological Laboratories, Nagoya. Japan), mouse anti-V5 monoclonal antibody: 6F5 (1:150; CTN3094, WAKO Chemical), and mouse anti-FLAG M2 (1:1000) (Sigma-Aldrich Japan Corp., Tokyo, Japan). Secondary antibodies were anti-mouse, anti-rabbit and/or anti-rat antibodies labeled with Alexa Fluor 488, 586 and 647 (1:300) (Life Technologies, Carlsbad, CA, USA). F-actin was stained by phalloidin conjugated with Alexa Fluor 568 (Life Technologies, Carlsbad, CA, USA). Images of samples were recorded using an FV1000 confocal microscope (PlanApo N 60× 1.42 NA objective lens; Olympus, Tokyo, Japan) or FV3000 confocal microscope (UPlanSApo 60×S2 1.30 NA objective lens; Olympus, Tokyo, Japan). To minimize bleed-through, each signal in the double- or triple-stained samples was imaged sequentially. Images were processed in accordance with the Guidelines for Proper Digital Image Handling using ImageJ and Affinity photo. For the quantification of the intensity of Rh1 staining in photoreceptor cytoplasm, we used more than 3 mosaic retinas with more than 8 wild-type and more than 6 mutant photoreceptors in each retina. Area of cytoplasm or whole cells and also their staining intensities were measured by Fiji (Schindelin et al., 2012).

Electron microscopy

Electron microscopy was performed as described previously (Satoh et al., 1997). Samples were observed under a JEM1400 electron microscope (JEOL, Tokyo, Japan), and montages were prepared with a CCD camera system (JEOL). The phenotypes were investigated using the section with the depth where a couple of photoreceptor nucleus within ommatidia were observed.

Competing Interests

All authors have read and approved this work and declare that they have no financial conflicts of interest.

Author contributions

Conceptualization: A.K.S.; Investigation: H.Y., Y.O., Y.Y., S.S., T.T.; Writing: T.S., A.K.S.; Supervision: T.S., A.K.S.; Project administration: A.K.S.; Funding acquisition: A.K.S., T.S., T.T.

Funding

This work was supported by Precursory Research for Embryonic Science and Technology (grant no. 25-J-J4215), Core Research for Organelle Diseases in Hiroshima University, Takeda Science Foundation, Ohsumi Frontier Science Foundation, Core Research for Evolutional Science and Technology (grant no. JPMJCR22E2), KAKENHI [grant nos. 15K07050, 19K06663 and 22H02617] to A.S., KAKENHI [grant no. 19K06566] to T.S, JST SPRING, grant no. JPMJSP2132] to T.T.

Acknowledgments

We thank Drs. A. Nakamura, J. Han, and Y. Inoue for kindly providing reagents. We also thank the Bloomington Drosophila Stock Center (Indiana University, IN, USA) and Kyoto Drosophila Stock Center (Kyoto Institute of Technology, Kyoto, Japan) for their fly stocks. We would like to thank Editage (www.editage.jp) for English language editing.

References

Acharya, U., Mowen, M. B., Nagashima, K. and Acharya, J. K. (2004). Ceramidase expression facilitates membrane turnover and endocytosis of rhodopsin in photoreceptors. *Proc Natl Acad Sci U S A* **101**, 1922-6.

Alloway, P. G., Howard, L. and Dolph, P. J. (2000). The formation of stable rhodopsin-arrestin complexes induces apoptosis and photoreceptor cell degeneration. *Neuron* **28**, 129-38.

Ang, A. L., Taguchi, T., Francis, S., Fölsch, H., Murrells, L. J., Pypaert, M., Warren, G. and Mellman, I. (2004). Recycling endosomes can serve as intermediates during transport from the Golgi to the plasma membrane of MDCK cells. *J Cell Biol* **167**, 531-43.

Beronja, S., Laprise, P., Papoulas, O., Pellikka, M., Sisson, J. and Tepass, U. (2005). Essential function of Drosophila Sec6 in apical exocytosis of epithelial photoreceptor cells. *J Cell Biol* **169**, 635-46.

Bhattacharya, S., Stewart, B. A., Niemeyer, B. A., Burgess, R. W., McCabe, B. D., Lin, P., Boulianne, G., O'Kane, C. J. and Schwarz, T. L. (2002). Members of the synaptobrevin/vesicle-associated membrane protein (VAMP) family in Drosophila are functionally interchangeable in vivo for neurotransmitter release and cell viability. *Proc Natl Acad Sci U S A* **99**, 13867-72.

Broadie, K., Prokop, A., Bellen, H. J., O'Kane, C. J., Schulze, K. L. and Sweeney, S. T. (1995). Syntaxin and synaptobrevin function downstream of vesicle docking in Drosophila. *Neuron* **15**, 663-73.

Chinchore, Y., Mitra, A. and Dolph, P. J. (2009). Accumulation of rhodopsin in late endosomes triggers photoreceptor cell degeneration. *PLoS Genet* **5**, e1000377.

Deitcher, D. L., Ueda, A., Stewart, B. A., Burgess, R. W., Kidokoro, Y. and Schwarz, T. L. (1998). Distinct requirements for evoked and spontaneous release of neurotransmitter are revealed by mutations in the Drosophila gene neuronal-synaptobrevin. *J Neurosci* **18**, 2028-39.

Deretic, D. (1997). Rab proteins and post-Golgi trafficking of rhodopsin in photoreceptor cells. *Electrophoresis* **18**, 2537-41.

Deretic, D., Huber, L. A., Ransom, N., Mancini, M., Simons, K. and Papermaster, D. S. (1995). rab8 in retinal photoreceptors may participate in rhodopsin transport and in rod outer segment disk morphogenesis. *J Cell Sci* **108 (Pt 1)**, 215-24.

Deretic, D. and Papermaster, D. S. (1993). Rab6 is associated with a compartment that transports rhodopsin from the trans-Golgi to the site of rod outer segment disk formation in frog retinal photoreceptors. *J Cell Sci* **106 (Pt 3)**, 803-13.

DiAntonio, A., Burgess, R. W., Chin, A. C., Deitcher, D. L., Scheller, R. H. and Schwarz, T. L. (1993). Identification and characterization of Drosophila genes for synaptic vesicle proteins. *J Neurosci* **13**, 4924-35.

Fujii, S., Kurokawa, K., Inaba, R., Hiramatsu, N., Tago, T., Nakamura, Y., Nakano, A., Satoh, T. and Satoh, A. K. (2020a). Recycling endosomes attach to the trans-side of Golgi stacks in. *J Cell Sci*.

Fujii, S., Tago, T., Sakamoto, N., Yamamoto, T., Satoh, T. and Satoh, A. K. (2020b). Recycling endosomes associate with Golgi stacks in sea urchin embryos. *Commun Integr Biol* **13**, 59-62.

Goldenring, J. R. (2015). Recycling endosomes. *Curr Opin Cell Biol* **35**, 117-22.

González-Méndez, L., Gradilla, A. C., Sánchez-Hernández, D., González, E., Aguirre-Tamaral, A., Jiménez-Jiménez, C., Guerra, M., Aguilar, G., Andrés, G., Falcón-Pérez, J. M. et al. (2020). Polarized sorting of Patched enables cytoneme-mediated Hedgehog reception in the Drosophila wing disc. *EMBO J* **39**, e103629.

Gordon, D. E., Chia, J., Jayawardena, K., Antrobus, R., Bard, F. and Peden, A. A. (2017). VAMP3/Syb and YKT6 are required for the fusion of constitutive secretory carriers with the plasma membrane. *PLoS Genet* **13**, e1006698.

Haberman, A., Williamson, W. R., Epstein, D., Wang, D., Rina, S., Meinertzhagen, I. A. and Hiesinger, P. R. (2012). The synaptic vesicle SNARE neuronal Synaptobrevin promotes endolysosomal degradation and prevents neurodegeneration. *J Cell Biol* **196**, 261-76.

Han, J., Reddig, K. and Li, H. S. (2007). Prolonged G(q) activity triggers fly rhodopsin endocytosis and degradation, and reduces photoreceptor sensitivity. *EMBO J* **26**, 4966-73.

Hebbar, S., Schuhmann, K., Shevchenko, A. and Knust, E. (2020). Hydroxylated sphingolipid biosynthesis regulates photoreceptor apical domain morphogenesis. *J Cell Biol* **219**.

Iwanami, N., Nakamura, Y., Satoh, T., Liu, Z. and Satoh, A. K. (2016). Rab6 Is Required for Multiple Apical Transport Pathways but Not the Basolateral Transport Pathway in Drosophila Photoreceptors. *PLoS Genet* **12**, e1005828.

Jahn, R. and Scheller, R. H. (2006). SNAREs--engines for membrane fusion. *Nat Rev Mol Cell Biol* **7**, 631-43.

Jin, E. J., Kiral, F. R., Ozel, M. N., Burchardt, L. S., Osterland, M., Epstein, D., Wolfenberg, H., Prohaska, S. and Hiesinger, P. R. (2018). Live Observation of Two Parallel Membrane Degradation Pathways at Axon Terminals. *Curr Biol* **28**, 1027-1038.e4.

Kakakhel, M., Tebbe, L., Makia, M. S., Conley, S. M., Sherry, D. M., Al-Ubaidi, M. R. and Naash, M. I. (2020). Syntaxin 3 is essential for photoreceptor outer segment protein trafficking and survival. *Proc Natl Acad Sci U S A* **117**, 20615-20624.

Kamalesh, K., Trivedi, D., Toscano, S., Sharma, S., Kolay, S. and Raghu, P. (2017). Phosphatidylinositol 5-phosphate 4-kinase regulates early endosomal dynamics during clathrin-mediated endocytosis. *J Cell Sci* **130**, 2119-2133.

Kandachar, V., Tam, B. M., Moritz, O. L. and Deretic, D. (2018). An interaction network between the SNARE VAMP7 and Rab GTPases within a ciliary membrane-targeting complex. *J Cell Sci* **131**.

Kiselev, A., Socolich, M., Vinós, J., Hardy, R. W., Zuker, C. S. and Ranganathan, R. (2000). A molecular pathway for light-dependent photoreceptor apoptosis in Drosophila. *Neuron* **28**, 139-52.

Klumperman, J. (2011). Architecture of the mammalian Golgi. *Cold Spring Harb Perspect Biol* **3**.

Kondylis, V. and Rabouille, C. (2003). A novel role for dp115 in the organization of tER sites in Drosophila. *J Cell Biol* **162**, 185-98.

Laffafian, A. and Tepass, U. (2019). Identification of Genes Required for Apical Protein Trafficking in. *G3 (Bethesda)* **9**, 4007-4017.

Langemeyer, L., Fröhlich, F. and Ungermann, C. (2018). Rab GTPase Function in Endosome and Lysosome Biogenesis. *Trends Cell Biol* **28**, 957-970.

Li, B. X., Satoh, A. K. and Ready, D. F. (2007). Myosin V, Rab11, and dRip11 direct apical secretion and cellular morphogenesis in developing Drosophila photoreceptors. *J Cell Biol* **177**, 659-69.

Littleton, J. T., Chapman, E. R., Kreber, R., Garment, M. B., Carlson, S. D. and Ganetzky, B. (1998). Temperature-sensitive paralytic mutations demonstrate that synaptic exocytosis requires SNARE complex assembly and disassembly. *Neuron* **21**, 401-13.

Lock, J. G. and Stow, J. L. (2005). Rab11 in recycling endosomes regulates the sorting and basolateral transport of E-cadherin. *Mol Biol Cell* **16**, 1744-55.

Malsam, J., Kreye, S. and Söllner, T. H. (2008). Membrane fusion: SNAREs and regulation. *Cell Mol Life Sci* **65**, 2814-32.

Mayor, S., Presley, J. F. and Maxfield, F. R. (1993). Sorting of membrane components from endosomes and subsequent recycling to the cell surface occurs by a bulk flow process. *J Cell Biol* **121**, 1257-69.

Mazelova, J., Ransom, N., Astuto-Gribble, L., Wilson, M. C. and Deretic, D. (2009). Syntaxin 3 and SNAP-25 pairing, regulated by omega-3 docosahexaenoic acid, controls the delivery of rhodopsin for the biogenesis of cilia-derived sensory organelles, the rod outer segments. *J Cell Sci* **122**, 2003-13.

Misaki, R., Morimatsu, M., Uemura, T., Waguri, S., Miyoshi, E., Taniguchi, N., Matsuda, M. and Taguchi, T. (2010). Palmitoylated Ras proteins traffic through recycling endosomes to the plasma membrane during exocytosis. *J Cell Biol* **191**, 23-9.

Mu, Y., Tian, Y., Zhang, Z. C. and Han, J. (2019). Metallophosphoesterase regulates light-induced rhodopsin endocytosis by promoting an association between arrestin and the adaptor protein AP2. *J Biol Chem* **294**, 12892-12900.

Orem, N. R., Xia, L. and Dolph, P. J. (2006). An essential role for endocytosis of rhodopsin through interaction of visual arrestin with the AP-2 adaptor. *J Cell Sci* **119**, 3141-8.

Otsuka, Y., Satoh, T., Nakayama, N., Inaba, R., Yamashita, H. and Satoh, A. K. (2019). Parcas is the predominant Rab11-GEF for rhodopsin transport in. *J Cell Sci* **132**.

Papanikou, E. and Glick, B. S. (2014). Golgi compartmentation and identity. *Curr Opin Cell Biol* **29**, 74-81.

Pinal, N. and Pichaud, F. (2011). Dynamin- and Rab5-dependent endocytosis is required to prevent Drosophila photoreceptor degeneration. *J Cell Sci* **124**, 1564-70.

Pocha, S. M., Shevchenko, A. and Knust, E. (2011). Crumbs regulates rhodopsin transport by interacting with and stabilizing myosin V. *J Cell Biol* **195**, 827-38.

Rao, S. S., Stewart, B. A., Rivlin, P. K., Vilinsky, I., Watson, B. O., Lang, C., Boulianne, G., Salpeter, M. M. and Deitcher, D. L. (2001). Two distinct effects on neurotransmission in a temperature-sensitive SNAP-25 mutant. *EMBO J* **20**, 6761-71.

Rister, J. and Heisenberg, M. (2006). Distinct functions of neuronal synaptobrevin in developing and mature fly photoreceptors. *J Neurobiol* **66**, 1271-84.

Rosenbaum, E. E., Vasiljevic, E., Cleland, S. C., Flores, C. and Colley, N. J. (2014). The Gos28 SNARE protein mediates intra-Golgi transport of rhodopsin and is required for photoreceptor survival. *J Biol Chem* **289**, 32392-409.

Satoh, A., Tokunaga, F., Kawamura, S. and Ozaki, K. (1997). In situ inhibition of vesicle transport and protein processing in the dominant negative Rab1 mutant of Drosophila. *J Cell Sci* **110 (Pt 23)**, 2943-53.

Satoh, A. K., O'Tousa, J. E., Ozaki, K. and Ready, D. F. (2005). Rab11 mediates post-Golgi trafficking of rhodopsin to the photosensitive apical membrane of Drosophila photoreceptors. *Development* **132**, 1487-97.

Satoh, A. K. and Ready, D. F. (2005). Arrestin1 mediates light-dependent rhodopsin endocytosis and cell survival. *Curr Biol* **15**, 1722-33.

Satoh, T., Inagaki, T., Liu, Z., Watanabe, R. and Satoh, A. K. (2013). GPI biosynthesis is essential for rhodopsin sorting at the trans-Golgi network in Drosophila photoreceptors. *Development* **140**, 385-94.

Satoh, T., Nakamura, Y. and Satoh, A. K. (2016). The roles of Syx5 in Golgi morphology and Rhodopsin transport in Drosophila photoreceptors. *Biol Open* **5**, 1420-1430.

Schindelin, J., Arganda-Carreras, I., Frise, E., Kaynig, V., Longair, M., Pietzsch, T., Preibisch, S., Rueden, C., Saalfeld, S., Schmid, B. et al. (2012). Fiji: an open-source platform for biological-image analysis. *Nat Methods* **9**, 676-82.

Shieh, B. H., Kristaponyte, I. and Hong, Y. (2014). Distinct roles of arrestin 1 protein in photoreceptors during Drosophila development. *J Biol Chem* **289**, 18526-34.

Taguchi, T. (2013). Emerging roles of recycling endosomes. *J Biochem* **153**, 505-10.

Thakur, R., Panda, A., Coessens, E., Raj, N., Yadav, S., Balakrishnan, S., Zhang, Q., Georgiev, P., Basak, B., Pasricha, R. et al. (2016). Phospholipase D activity couples plasma membrane endocytosis with retromer dependent recycling. *Elife* **5**.

Wandinger-Ness, A. and Zerial, M. (2014). Rab proteins and the compartmentalization of the endosomal system. *Cold Spring Harb Perspect Biol* **6**, a022616.

Wang, D., Epstein, D., Khalaf, O., Srinivasan, S., Williamson, W. R., Fayyazuddin, A., Quiocho, F. A. and Hiesinger, P. R. (2014a). Ca2+-Calmodulin regulates SNARE assembly and spontaneous neurotransmitter release via v-ATPase subunit V0a1. *J Cell Biol* **205**, 21-31.

Wang, D. and Hiesinger, P. R. (2012). Autophagy, neuron-specific degradation and neurodegeneration. *Autophagy* **8**, 711-3.

Wang, S., Tan, K. L., Agosto, M. A., Xiong, B., Yamamoto, S., Sandoval, H., Jaiswal, M., Bayat, V., Zhang, K., Charng, W. L. et al. (2014b). The retromer complex is required for rhodopsin recycling and its loss leads to photoreceptor degeneration. *PLoS Biol* **12**, e1001847.

Xiong, B., Bayat, V., Jaiswal, M., Zhang, K., Sandoval, H., Charng, W. L., Li, T., David, G., Duraine, L., Lin, Y. Q. et al. (2012). Crag is a GEF for Rab11 required for rhodopsin trafficking and maintenance of adult photoreceptor cells. *PLoS Biol* **10**, e1001438.

Xiong, B. and Bellen, H. J. (2013). Rhodopsin homeostasis and retinal degeneration: lessons from the fly. *Trends Neurosci* **36**, 652-60.

Xu, T. and Rubin, G. M. (1993). Analysis of genetic mosaics in developing and adult Drosophila tissues. *Development* **117**, 1223-37.

Xu, X. Z., Wes, P. D., Chen, H., Li, H. S., Yu, M., Morgan, S., Liu, Y. and Montell, C. (1998). Retinal targets for calmodulin include proteins implicated in synaptic transmission. *J Biol Chem* **273**, 31297-307.

Yamanaka, N., Marqués, G. and O'Connor, M. B. (2015). Vesicle-Mediated Steroid Hormone Secretion in Drosophila melanogaster. *Cell* **163**, 907-19.

Yamashiro, D. J. and Maxfield, F. R. (1987). Acidification of morphologically distinct endosomes in mutant and wild-type Chinese hamster ovary cells. *J Cell Biol* **105**, 2723-33.

Yamazaki, Y., Palmer, L., Alexandre, C., Kakugawa, S., Beckett, K., Gaugue, I., Palmer, R. H. and Vincent, J. P. (2016). Godzilla-dependent transcytosis promotes Wingless signalling in Drosophila wing imaginal discs. *Nat Cell Biol* **18**, 451-7.

Yonamine, I., Bamba, T., Nirala, N. K., Jesmin, N., Kosakowska-Cholody, T., Nagashima, K., Fukusaki, E., Acharya, J. K. and Acharya, U. (2011). Sphingosine kinases and their metabolites modulate endolysosomal trafficking in photoreceptors. *J Cell Biol* **192**, 557-67.

Yoshihara, M., Ueda, A., Zhang, D., Deitcher, D. L., Schwarz, T. L. and Kidokoro, Y. (1999). Selective effects of neuronal-synaptobrevin mutations on transmitter release evoked by sustained versus transient Ca2+ increases and by cAMP. *J Neurosci* **19**, 2432-41.

Zhao, X., Yang, H., Liu, W., Duan, X., Shang, W., Xia, D. and Tong, C. (2015). Sec22 regulates endoplasmic reticulum morphology but not autophagy and is required for eye development in Drosophila. *J Biol Chem* **290**, 7943-51.

Figures

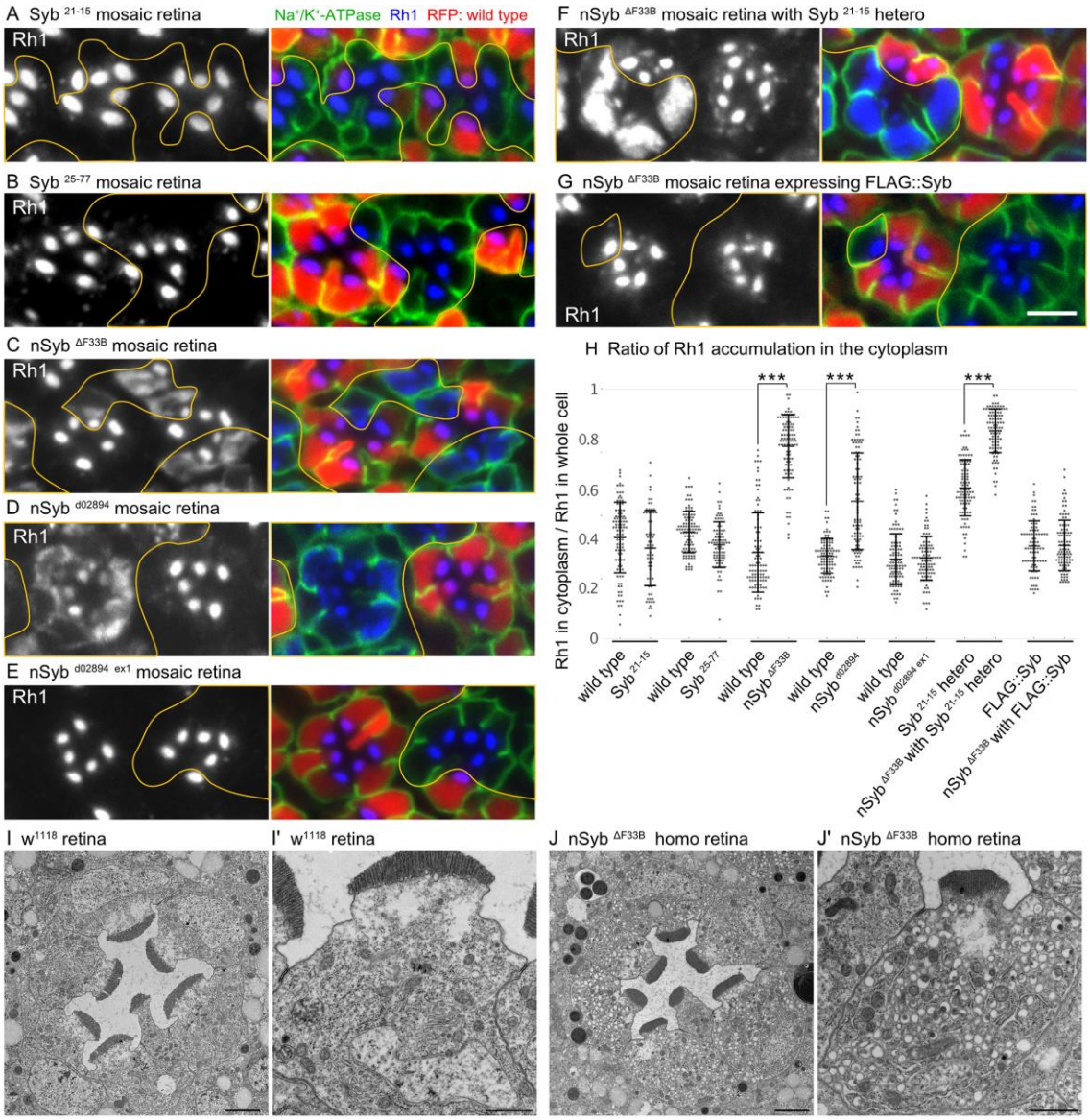

Fig. 1. Rhabdomere transport is impaired in nSyb-deficient photoreceptors.

(A-E) Immunostaining of *Syb*$^{21-15}$ (A), *Syb*$^{25-77}$ (B), *nSyb*$^{\Delta F33B}$ (C), *nSyb*^{d02894} (D), or *nSyb*$^{d02894\ ex1}$ (E) mosaic retinas with anti-Na^+/K^+-ATPase-α (green) and anti-Rh1 (blue) antibodies. RFP (red) shows wild-type cells.

(F, G) Immunostaining of *nSyb*$^{\Delta F33B}$ mosaic retinas with a single *Syb*$^{21-15}$ chromosome (F) or expressing FLAG::Syb (G) with anti-Na^+/K^+-ATPase-α (green) and anti-Rh1 (blue) antibodies. RFP (red) shows *Syb*$^{21-15}$ heterozygous (F) or FLAG::Syb expressing cells (G) without *nSyb*$^{\Delta F33B}$ alleles.

(H) The ratio of the integrated density of Rh1 staining of the cytoplasm compared to that of whole cells. Measurements from wild-type and mutant cells in mosaic retina are shown as pairs, indicated by bars under the plots. Error bars indicate the standard deviation. Significance according to two-tailed unpaired Student's *t*-test: ***$p < 0.001$.
(I, J) Electron micrographs of w^{1118} (I, I') or $nSyb^{\Delta F33B}$ (J, J') ommatidia (I, J) and photoreceptors (I', J') from late pupal flies. w^{1118} is the wild-type except for eye color. Scale bar: 5 μm (A–G), 2 μm (I, J), and 1 μm (I', J').

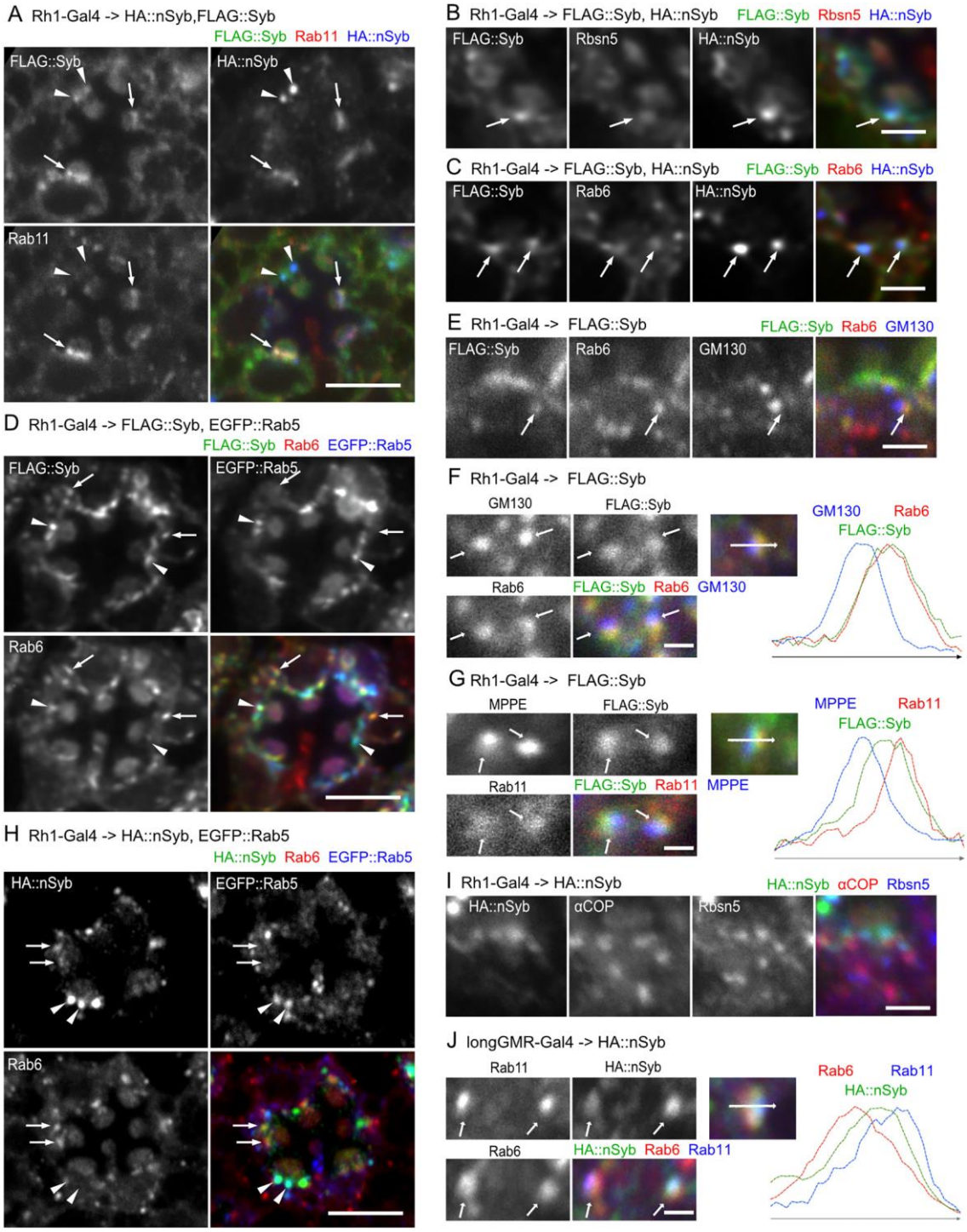

Fig. 2. nSyb and Syb localize on post-Golgi vesicles and endocytic compartments. (A-C) Immunostaining of wild-type retinas expressing FLAG::Syb and HA::nSyb by Rh1-Gal4. (A) anti-FLAG (green), anti-Rab11 (red), and anti-HA (blue) antibodies; (B) anti-FLAG (green), anti-Rbsn5 (red), and anti-HA (blue) antibodies; and (C) anti-FLAG (green), anti-Rab6 (red), and anti-HA (blue) antibodies.

(D) Immunostaining of wild-type retinas expressing FLAG::Syb and EGFP::Rab5 (shown in blue) by Rh1-Gal4, using anti-FLAG (green) and anti-Rab6 (red) antibodies.
(E-G) Immunostaining of wild-type retinas expressing FLAG::Syb by Rh1-Gal4. (E, F) Anti-FLAG (green), anti-Rab6 (red), and anti-GM130 (blue) antibodies; and (G) anti-FLAG (green), anti-Rab11 (red), and anti-MPPE (blue) antibodies. Right plots of signal intensities from image on the left. Signal intensity was measured along the 1.5 μm arrow in inset, graph shows the overlap between channels (F, G).
(H) Immunostaining of wild-type retinas expressing HA::nSyb and EGFP::Rab5 (shown in blue) by Rh1-Gal4, using anti-HA (green) and anti-Rab6 (red) antibodies.
(I) Immunostaining of wild-type retinas expressing HA::nSyb by Rh1-Gal4, using anti-HA (green), anti-αCOP (red), and anti-Rbsn5 (blue) antibodies.
(J) Immunostaining of wild-type retinas expressing HA::nSyb by longGMR-Gal4, using anti-HA (green), anti-Rab6 (red), and anti-Rab11 (blue) antibodies. Right plots of signal intensities from image on the left. Signal intensity was measured along the 1.5 μm arrow in inset, graph shows the overlap between channels.
Scale bar: 5 μm (A, D, H), 2 μm (B, C, E, I), and 1 μm (F, G, J).

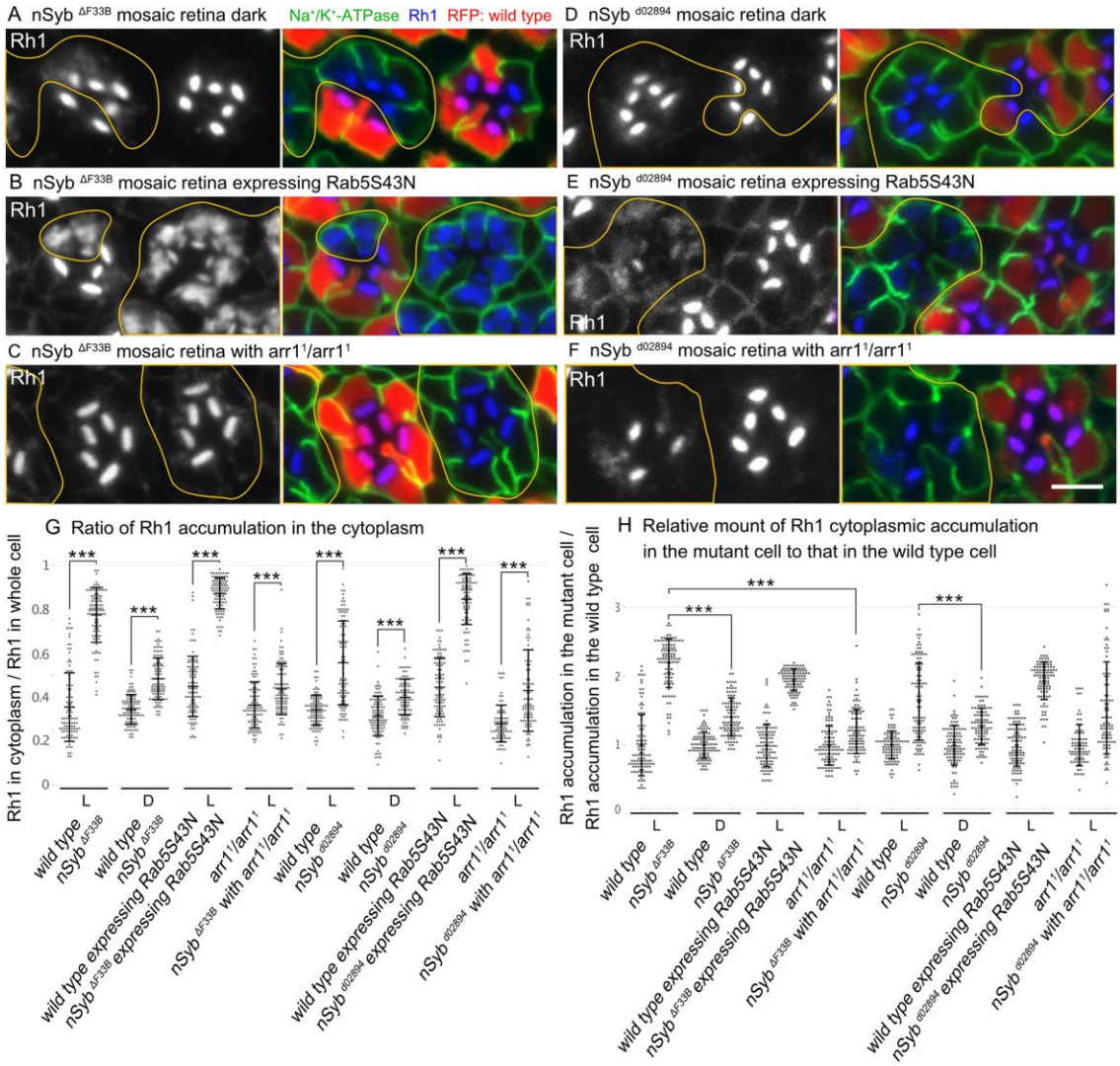

Fig. 3. Rh1 accumulation in nSyb-deficient cells depends on the activity of Rh1 endocytosis.

Immunostaining of mosaic retinas with the indicated genotypes using anti-Na^+/K^+-ATPase-α (green) and anti-Rh1 (blue) antibodies. RFP (red) represents wild-type cells.

(A) Dark-raised *nSyb*$^{\Delta F33B}$ mosaic retinas.

(B, C) *nSyb*$^{\Delta F33B}$ mosaic retinas expressing Rab5S43N (B) or those with *arr1*^{1}/*arr1*^{1}(C).

(D) Dark-raised *nSyb* ^{d02894} mosaic retinas.

(E, F) *nSyb* ^{d02894} mosaic retinas expressing Rab5S43N (E) or those with *arr1*^{1}/*arr1*^{1}(F).

(G, H) The ratio of integrated fluorescence density for Rh1 staining of the cytoplasm compared to that of whole cells was plotted (G). The relative integrated density for Rh1 staining of the cytoplasm against that of whole cells was plotted with the wild type as 1

(H). Measurements from wild-type and mutant cells in mosaic retina are shown as pairs, indicated by bars under the plots. L or D indicate flies reared in light (L) or dark (D) conditions, respectively. Error bars indicate the standard deviation. Significance according to two-tailed unpaired Student's *t*-test: ***$p < 0.001$.

Scale bar: 5 μm (A-F).

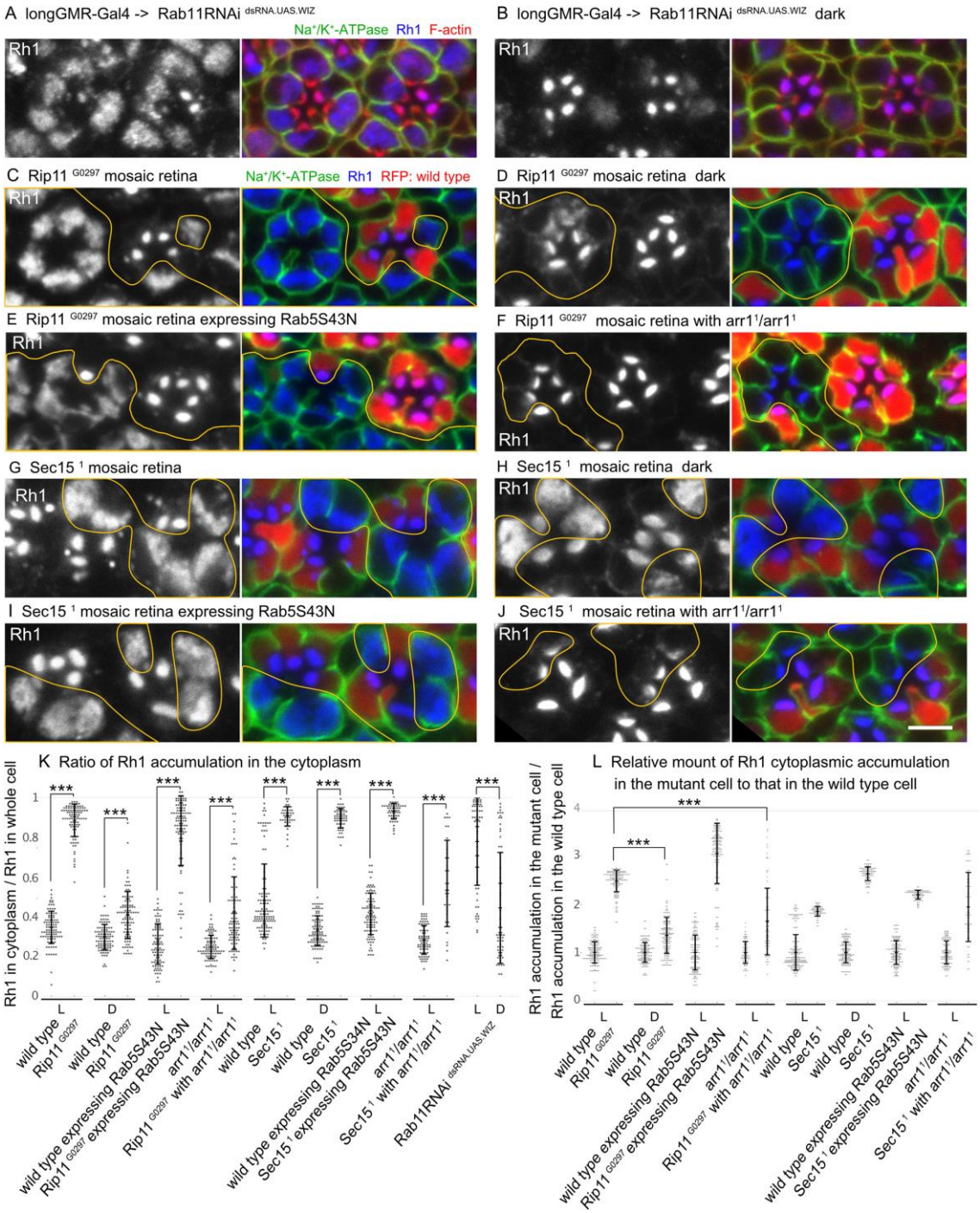

Fig. 4. Rh1 accumulation in Rab11-, Rip11-, and Sec15-deficient cells depends on the activity of Rh1 endocytosis.

Immunostaining of mosaic retinas with the indicated genotypes using anti-Na^+/K^+-ATPase-α (green) and anti-Rh1 (blue) antibodies. F-actin is stained with phalloidin (red) (A, B). RFP (red) indicates the wild-type cells (C-J).

(A, B) LongGMR-Gal4 driven Rab11RNAi-expressing retinas from flies reared in light (A) or dark conditions (B).
(C, D) *Rip11*^{G0297} mosaic retinas from flies reared in light (C) or dark conditions (D).
(E, F) *Rip11*^{G0297} mosaic retinas expressing Rab5S43N (E) or those with *arr1*^{1}/*arr1*^{1}(F).
(G, H) *Sec15*^{1} mosaic retinas from flies reared in light (G) or dark conditions (H).
(I, J) *Sec15*^{1} mosaic retinas expressing Rab5S43N (I) or those with *arr1*^{1}/*arr1*^{1}(J).
(K, L) The ratio of integrated density for Rh1 staining in the cytoplasm against that of whole cells was plotted (K). The relative integrated density for Rh1 staining in the cytoplasm against that of whole cells was plotted with the wild type as 1 (L). Measurements from wild-type and mutant cells in mosaic retina are shown as pairs, indicated by bars under the plots. L or D indicate flies reared in light (L) or dark (D) conditions, respectively. Error bars indicate the standard deviation. Significance according to two-tailed unpaired Student's *t*-test: ***$p < 0.001$.
Scale bar: 5 μm (A-J).

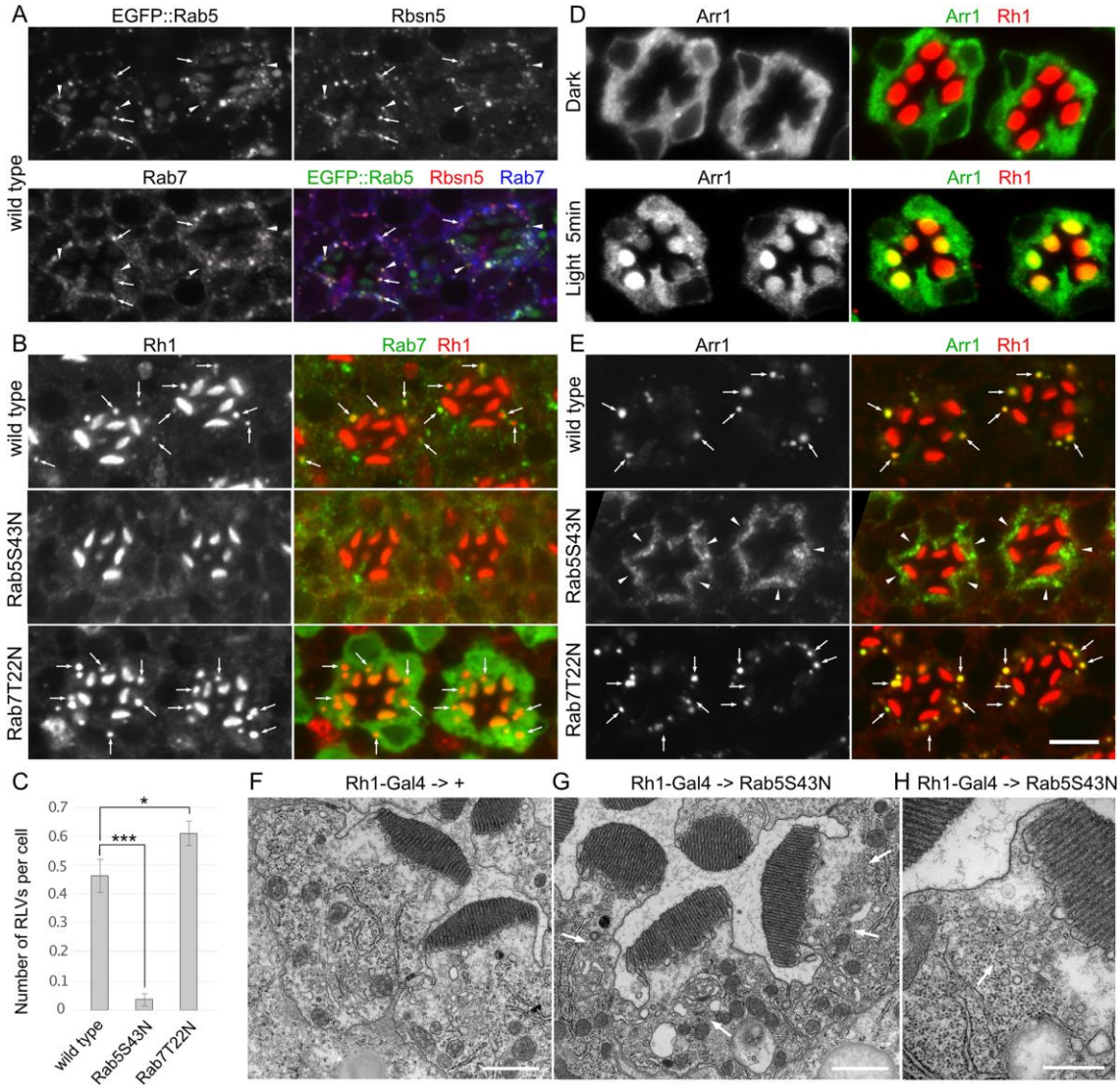

Fig. 5. nSyb and Syb localize on post-Golgi vesicles and endocytic compartments.

(A) Immunostaining of wild-type retinas expressing EGFP::Rab5 (green) by Rh1-Gal4, using anti-Rbsn5 (red), and anti-Rab7 (blue) antibodies. Arrows indicate the vesicles positive for EGFP::Rab5, Rbsn5, and Rab7. Arrowheads indicate EGFP::Rab5 and Rbsn5 positive, but Rab7 negative vesicles.

(B) Immunostaining of wild-type retinas without (upper panel) or with the expression of Rab5S43N (middle panel) or Rab7T22N (lower panel) by Rh1-Gal4, using anti-Rab7 (green) and anti-Rh1 (red) antibodies. Arrows indicate Rh1-containing large vesicles (RLVs).

(C) The plot for the number of Rh1-containing large vesicles (RLVs) per photoreceptor. Error bars indicate the standard deviation with three retinas. Significance according to two-tailed unpaired Student's t-test: ***$p < 0.001$; *$p < 0.05$.

(D) Immunostaining of dark-reared wild-type retinas, dissected in dark or in light, using anti-Arr1 (green) and anti-Rh1 (red) antibodies.

(E) Immunostaining of wild-type retinas without (upper panel) or with the expression of Rab5S43N (middle panel) or Rab7T22N (lower panel) by Rh1-Gal4, using anti-Arr1 (green) and anti-Rh1 (red) antibodies. Arrows and arrowheads indicate Rh1-containing large vesicles (RLVs) and small vesicles.

(F) Electron micrograph of wild-type photoreceptors.

(G, H) Electron micrographs of photoreceptors expressing Rab5S43N by Rh1-Gal4. Arrows indicate accumulated small vesicles.

Scale bar: 5 μm (A, B, D, E), 1 μm (F, G), and 500 nm (H).

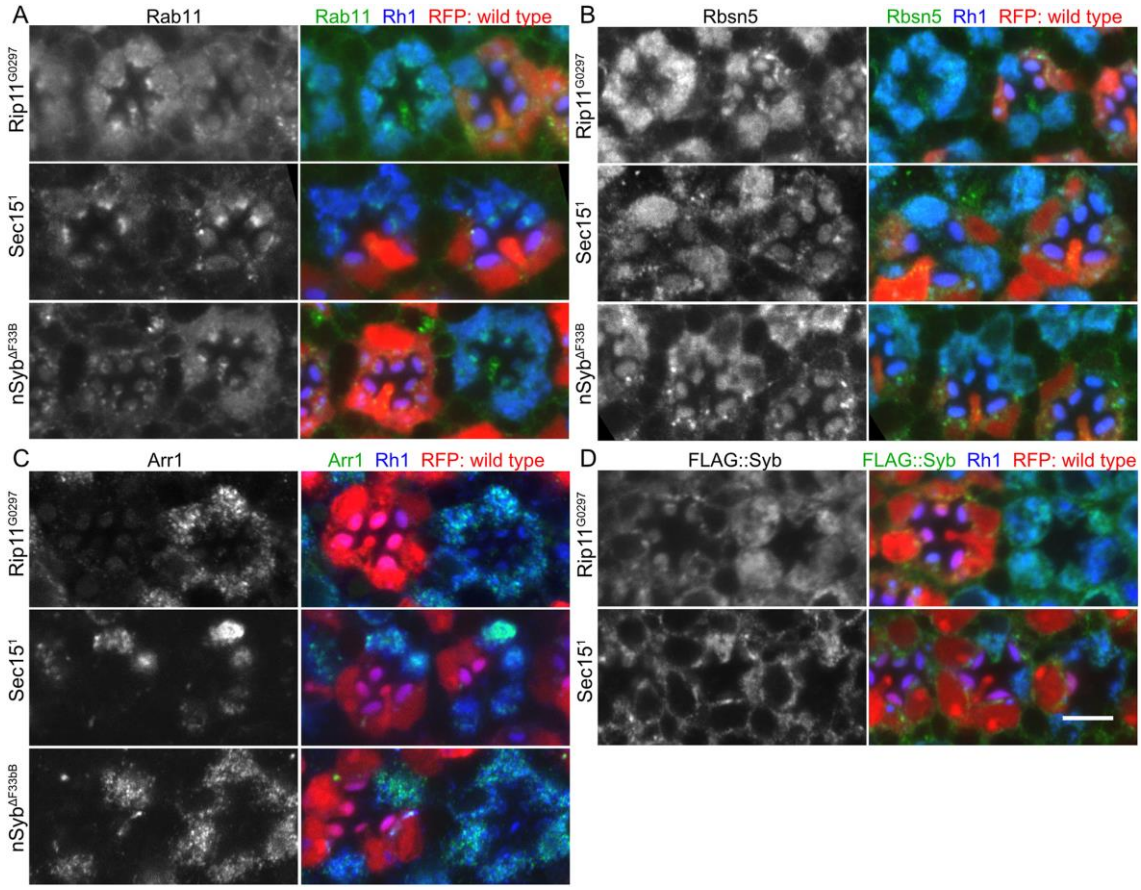

Fig. 6. Exocytic and endocytic Rh1 accumulate together in the cytoplasm of Rip11-, Sec15-, or nSyb-deficient cells.

(A-C) Immunostaining of *Rip11*^{G0297}, *Sec15*^{1}, or *nSyb*$^{\Delta F33B}$ mosaic retinas with the indicated antibodies. RFP (red) represents the wild-type cells. (A) Anti-Rab11 (green) and anti-Rh1 (blue) antibodies. (B) Anti-Rbsn5 (green) and anti-Rh1 (blue) antibodies. (C) Anti-Arr1 (green) and anti-Rh1 (blue) antibodies.

(D) Immunostaining of *Rip11*^{G0297} or *Sec15*^{1} mosaic retinas expressing FLAG::Syb by Rh1-Gal4. Anti-FLAG (green) and anti-Rh1 (blue) antibodies. RFP (red) represents wild-type cells.

Scale bar: 5 μm (A–D).

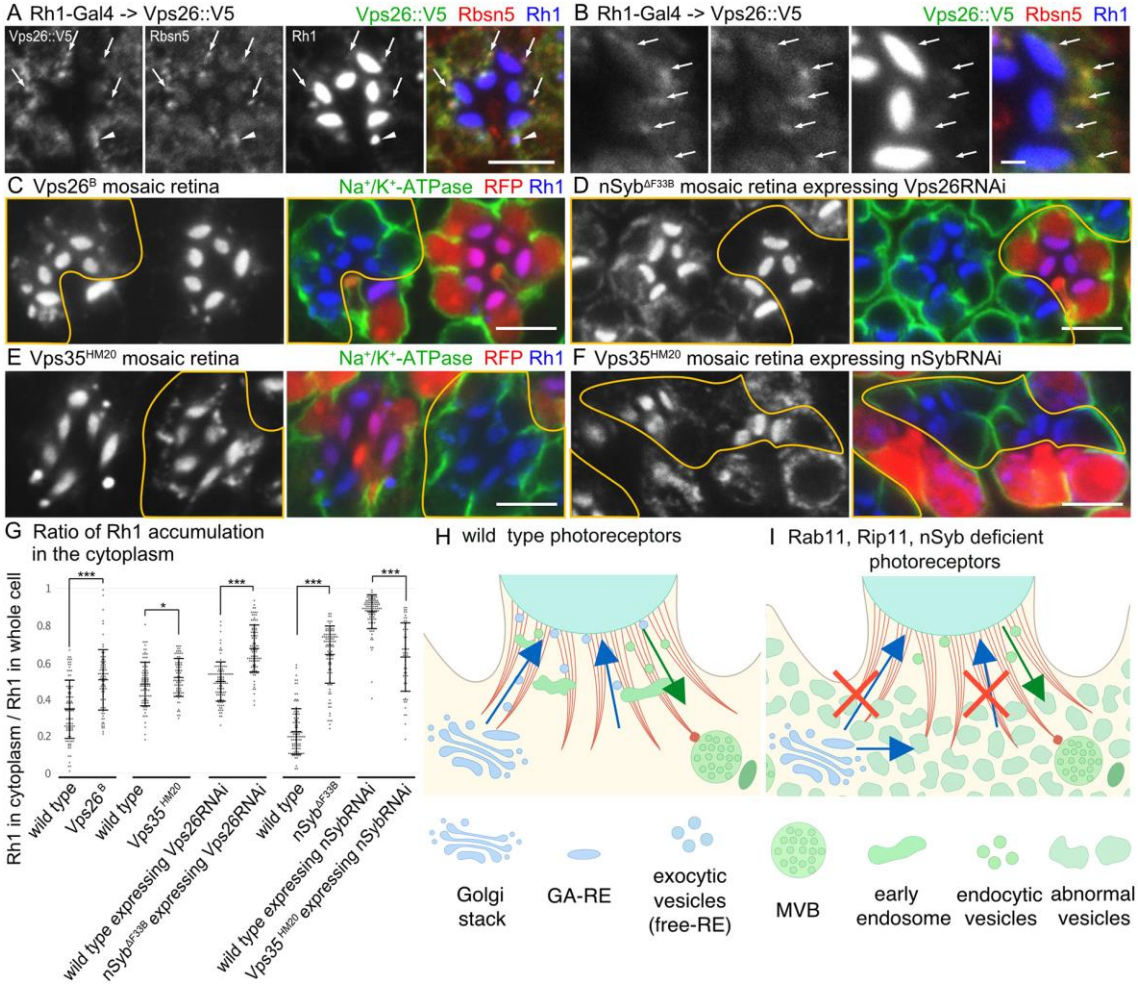

Fig. 7. Epistatic analysis of retromer and nSyb.

(A, B) Immunostaining of wild-type retinas expressing Vps26::V5 by Rh1-Gal4, anti-V5 (green), anti-Rbsn5 (red), and anti-Rh1 (blue) antibodies.

(C-F) Immunostaining of mosaic retinas with the indicated genotypes using anti-Na^+/K^+-ATPase-α (green) and anti-Rh1 (blue) antibodies. RFP (red) represents wild-type cells. *Vps26*^{B} mosaic retina (C), *nSyb*$^{\Delta F33B}$ mosaic retina expressing Vps26RNAi^{HMS01768} by longGMR-Gal4 (D), *Vps35*^{HM20} mosaic retina (E), *Vps35*^{HM20} mosaic retina expressing nSybRNAi^{JFS03417} by longGMR-Gal4 (F). Scale bar: 5 μm (A), 1 μm (B), 5 μm (C–F).

(G) The ratio of the integrated density of Rh1 staining of the cytoplasm compared to that of whole cells. Measurements from wild-type and mutant cells in mosaic retina are shown as pairs, indicated by the bars under the plots. Error bars indicate the standard deviation. Significance according to two-tailed unpaired Student's *t*-test: ***$p < 0.001$; *$p < 0.05$.

(H, I) Models for Rh1 transport in the wild-type photoreceptors (H) and Rab11-, Rip11-, or nSyb-deficient photoreceptors (I). Exocytic and endocytic organelles are shown in blue and green, respectively. F-actin in the retinal terminal web (RTW) and actin-patch attached to the multivesicular body (MVB) are shown in red. Abnormal vesicles with Rh1 accumulated in Rab11-, Rip11-, or nSyb-deficient photoreceptors are shown in turquoise. In the wild-type photoreceptors, newly synthesized Rh1 travels through the Golgi stack and reaches GA-REs. Rh1 is then transported to rhabdomeres on free REs by the Rab11/Rip11/MyoV complex. Light-dependently endocytosed Rh1 first localizes in early endosomes. Some of this Rh1 is incorporated into free RE and then recycled back to rhabdomeres, whereas the remaining is transported to MVBs and degraded. nSyb is transported on GA-REs and free REs together with Rh1 and induces the fusion of free REs with the rhabdomere base membrane. In Rab11-, Rip11-, or nSyb-deficient photoreceptors, free REs mingle with early endosomes and form abnormal vesicles. These vesicles contain Rh1 from Golgi stacks as well as Rh1 endocytosed from rhabdomeres.